An Energy Transfer Study of Homopolymer Localization in Block Copolymers

Yahya Rharbi, Jian-Xin Zhang,† John G. Spiro, Liusheng Chen,‡ and Mitchell A. Winnik*

Department of Chemistry, University of Toronto, 80 St. George St., Toronto, Ontario, Canada M5S 3H6

J. D. Vavasour and M. D. Whitmore

Department of Physics and Physical Oceanography, Memorial University of Newfoundland, St. John's, Newfoundland, Canada A1B 3X7

R. Jérôme

Center for Education and Research on Macromolecules, University of Liège, Sart-Tilman B6, 4000 Liège, Belgium

Received June 19, 2002

ABSTRACT: We have investigated the localization of homopolystyrene (hPS) in its blends with poly(styrene-*b*-butyl methacrylate) (PS-*b*-PBMA), at 140 °C, measuring the quantum efficiency of direct energy transfer (Φ_{ET} of DET) between hPS randomly labeled with phenanthrene moieties and PS-*b*-PBMA labeled at the junction with anthracene. The molecular weight of hPS was similar to the molecular weight of the PS block of PS-*b*-PBMA, and the hPS content was kept to a maximum of 26 vol %, to preserve the lamellar morphology of PS-*b*-PBMA. We have found very low rates of DET, which implies that hPS is almost totally localized between the PS brushes of PS-*b*-PBMA. In addition to the experimental measurements, we also calculated Φ_{ET} values by simulating fluorescence decay curves, based on Vavasour and Whitmore's numerical self-consistent-field (NSCF) formalism. The latter theory confirmed that we were dealing with a "dry brush" situation, but the NSCF results suggested a higher level of penetration of hPS than the experiments. We attribute this discrepancy to uncertainties about inputs to the simulations, particularly the Flory−Huggins χ parameter and the Kuhn length for the PBMA block.

Introduction

Melts of diblock copolymers tend to self-assemble into a variety of microphase-separated, ordered structures, such as lamellae, spheres, and cylinders.[1] The nature of the ordered phase depends primarily on the ratio of the block lengths N_A and N_B. When the block copolymer is nearly symmetric (volume fraction of A ≈ volume fraction of B), and the product of the Flory−Huggins interaction parameter and the total block copolymer chain length is large ($\chi N \gg 10$, with $N = N_A + N_B$), the polymer forms a lamellar superstructure in which the A and B blocks are well-segregated and separated by a narrow interface.[2,3]

For many years, there has been a strong interest in the nature of homopolymer blends with diblock copolymers. One important aspect is the location of the homopolymer in blends rich in block copolymer.[4−11] The most extensive studies involved binary mixtures of poly(styrene-*b*-isoprene) (PS-*b*-PI) and polystyrene (hPS), examined both by the Hashimoto group[8] and by Winey and co-workers.[9,12] Russell and co-workers[13] examined blends of poly(styrene-*b*-methyl methacrylate) (PS-*b*-PMMA) with hPS. Orso and Green[14] have recently reported an atomic force microscopy (AFM) study on the same system. Experiments involving blends of poly(styrene-*b*-2-vinylpyridine) (PS-*b*-P2VP) plus hPS have been reported by Matsushita, Torikai, and co-workers.[15]

Hashimoto and co-workers[8] and Winey et al.[9,12] used a combination of small-angle X-ray scattering (SAXS) and transmission electron microscopy (TEM) to investigate changes in the lamellar morphology that result from blending hPS into PS-*b*-PI samples. They found that blends containing up to 20 wt % of hPS maintain a well-ordered lamellar structure. In these blends, the thickness of the PS microdomain increases with addition of hPS, whereas that of the PI decreases. The decrease of the PI domain size became less pronounced with increasing hPS molecular weight. For the case in which the molecular weights of the hPS and the PS block of the copolymer were comparable, $M_{hPS} \approx M_{PS}$, the thickness of the PI microdomain was not affected by the addition of the hPS, and the increase in the PS microdomain could be fully accounted for simply by the volume of the added hPS. When the hPS content exceeds 35 wt %, the morphology changes to hexagonally packed cylindrical microdomains. They concluded that short hPS ($M_{hPS} < M_{PS}$) dissolves in the PS microdomains of the block copolymer, and is distributed throughout them.[8b] Longer hPS chains, but still with $M_{hPS} < M_{PS}$, tend to localize in the centers of the PS microdomains.[8a] In samples in which $M_{hPS} \approx M_{PS}$, the hPS undergoes microphase separation and is confined primarily to the centers of the PS microdomains.[8d] Macrophase separation can also occur in these blends, especially when $M_{hPS} \gg M_{PS}$.[8d] Similar conclusions were reached by Matsushita and associates in their studies of PS-*b*-P2VP + hPS blends.[15]

† Current address: Polymer Source, Inc., 771 Lajoie, Dorval, Quebec, Canada H9P 1G7.

‡ Current address: Institute of Chemistry, Chinese Academy of Science, Beijing 1000080, China.

10.1021/ma020962l CCC: $25.00
Published on Web 01/18/2003

These are the results from which the concepts of "wet brush" and "dry brush" were developed. If one draws an analogy between a strongly segregated lamellar A/B diblock copolymer and a brush of polymer chains adsorbed to an impenetrable surface,[8,9,11,16] a "wet brush" would refer to the case in which there is substantial penetration of B homopolymer into the B microdomain. The term "dry brush" refers to the case in which the B homopolymer becomes localized between the B-blocks of adjacent brushes. Since the homopolymer does not penetrate into the microdomains formed by the block copolymer, the brush remains dry. As a consequence, one imagines that there is little probability that the homopolymer in a dry-brush blend will penetrate to the interface between the two blocks.[7−9]

We are interested in using direct nonradiative energy transfer (DET) experiments[17−19] to probe the distribution of homopolymers in their blends with diblock copolymers. This experiment is simple in conception and more difficult in execution. One can blend a donor-dye-labeled homopolymer with a diblock copolymer bearing an acceptor dye at a well-defined site such as the A/B junction or one of the chain ends. DET from the donor to the acceptor dye establishes proximity between the homopolymer and the locus of the labeled portion of the block copolymer. In the past, we have used DET experiments to probe the interface of block copolymer melts[20] and polymer blends.[21] Here we use DET experiments to examine the location of hPS in binary blends with a symmetric poly(styrene-*b*-butyl methacrylate) whose PS block is similar in length to the hPS. In these experiments, the hPS is labeled with phenanthrene (hPS-*Phe*) as the donor dye, and the block copolymer is labeled with an anthracene moiety at the junction (PS-*b(An)*-PBMA) as the acceptor dye. This pair allows us to examine the penetration of hPS into the PS-*b*-PBMA interface.

We are not the first to investigate the details of the distribution of homopolymer in diblock copolymer melts. For instance, Mayes, Russell, and co-workers[13] used specular neutron reflectivity (SNR) to obtain quantitative information on the distribution of PS and PMMA homopolymers in ordered thin films of symmetric PS-*b*-PMMA. Their model for analyzing SNR profiles included a hyperbolic tangent function for the segment distribution of the block copolymer across the interface. For the distribution of homopolymer, they considered two limiting possibilities: a narrow Gaussian distribution confined to the center of the like block and a uniform distribution throughout the corresponding block. In accord with studies on PS-*b*-PI, they found that low molecular weight homopolymer is distributed almost uniformly within the corresponding block copolymer domains. For homopolymer molecular weights similar to that of the corresponding copolymer block, they found localization of the homopolymers between the copolymer blocks.

Several groups have also predicted these results theoretically. Shull and Winey[12] used numerical mean-field calculations, with χN corresponding to the experimental conditions of Winey et al.[9] on hPS in PS-*b*-PI, to show that the highest segment density of added hPS occurs between the ends of the PS blocks. In this system, there is substantial penetration of hPS into the brush of PS chains. These calculations, which assume incompressibility and an infinitely thin interface, predict that the fraction of hPS reaching the interface is negligible for $N_{\mathrm{hPS}} = 1.37N_{\mathrm{PS}}$.

Matsen,[22] using numerical self-consistent-field (NSCF) calculations, was able to reproduce many of the results of Winey et al.[9] These calculations show how low-*M* hPS "spreads apart" the chains within the PS domain, increasing the interfacial area per copolymer, and allows the PI blocks of PS-*b*-PI to relax and the width of the PI domains to contract. We note that the PS-*b*-PI polymers studied by Winey et al. were strongly segregated, whereas Matsen's model treated weakly segregated blends. Banaszak and Whitmore[23] carried out model calculations on homopolymer−block copolymer blends using an approximation to NSCF theory for weak segregation. They were able to calculate the overall block copolymer domain thickness, the widths of the two subdomains, the lateral swelling of the copolymer domains by homopolymer, the localization of the homopolymers, and the density profiles for each component. Very recently, Vavasour and Whitmore[24] developed NSCF techniques that are appropriate to all segregation regimes. For the case of a B-homopolymer added to an A-*b*-B block copolymer, they were able to conduct detailed analyses of cases in which the added homopolymer induced an increase or decrease in the domain thickness. With a suitable choice of system parameters, especially the Flory χ parameter, they found excellent agreement with the experiments for both the neat copolymer and the blends.

We initially conceived the experiments described here as a further test of the Vavasour−Whitmore model[24] and its ability to predict penetration of homopolymer to the interface of a modestly segregated block copolymer. We take advantage of dye-labeled symmetric PS-*b*-PBMA samples synthesized by Zhang in Liège at the same time as he synthesized a broader series of samples (without dye, some labeled with deuterium) for studies reported over the past several years by the Stamm group.[25] Experiments by the Stamm group provide information on the period spacing as a function of chain length, values of the χ parameter, and information about the interface thickness as a function of temperature. We add donor-labeled polystyrene (hPS-*Phe*) homopolymer ($M_{\mathrm{hPS}} = 100\,000$) to samples of PS-*b*(*An*)-PBMA ($M_{\mathrm{PS}} = 92\,000$, $M_{\mathrm{PBMA}} = 91\,000$), which bears an acceptor dye at the junction and forms a periodic lamellar structure in the melt. We carried out NSCF calculations to obtain the distribution profiles for hPS segments and for the junctions of PS-*b*-PBMA, using the Flory−Huggins χ parameter 0.0098 reported by Schubert et al. for 140° C,[3,26a] defined with reference to the monomeric volume of styrene, taken to be 99.378 cm^3/mol.[26b] In more recent reports[26c,d] the Stamm group suggested a somewhat higher χ value, which we have considered in sensitivity studies, but the latter studies have not significantly affected our major conclusions. We use the NSCF profiles in combination with the theory of energy transfer to calculate the efficiency of energy transfer expected in this system. The DET experiment shows that no more than 4% of hPS penetrates into the interfacial zone of the copolymer, whereas SCF simulations performed with the literature values of χ predict that more than 20% of the hPS segments overlap the interfacial region. We conclude that the PS chains of the block copolymer lamellae form a much drier brush than predicted by the theory with these parameters. We end the paper with a discussion of the consistency of

this result with the conclusions of Vavasour and Whitmore on the existing measurements of interaction parameters.

Experimental Section

Polymer Synthesis and Characterization. Dye-labeled poly(styrene-*b*-butyl methacrylate) was prepared by anionic polymerization as described by Weidisch et al.[25b] The first step of the polymerization was modified as described by Hruska et al.: [27] Following polymerization of the PS block, 1.1 equiv of 1-(2-anthryl)-1-phenylethylene (source: S. Ni, University of Toronto) was added to the reaction prior to polymerization of the BMA block. M_{PS} was determined by gel permeation chromatography (GPC, hPS standards). The composition was established by ^{1}H NMR. GPC measurements with both refractive index and UV detection were used to calculate the polydispersity (M_w/M_n) and monitor the attachment of the dye to the polymer. In this way we determine that M_w(PS) = 92 000, M_w(PBMA) = 91 000, and the total molecular weight M_w = 183 000 with M_w/M_n = 1.04. The anthracene content of the copolymer was measured by UV−vis (using the extinction coefficient for 1-(2-anthryl)-1-phenylhexane as a model compound) and was found to be 5.6 μmol/g, corresponding to 1.0 anthracene group per molecule.

Phenanthrene-labeled hPS was synthesized from polystyrene purchased as a molecular weight standard (Sigma, M_w = 100 000, M_w/M_n = 1.06). It was chloromethylated using CH_3-$OCH_2CH_2OCH_2Cl$ (MEM-chloride, Aldrich) as a safer alternative to chloromethyl methyl ether, under standard conditions[28] ($ZnCl_2$ in chloroform), to introduce approximately 1 mol % chloromethyl groups. The purified polymer (repeated precipitation from toluene into methanol) was added to a solution containing 1.2 equiv of 9-hydroxymethylphenanthrene in dimethylformamide and treated with a slight excess of sodium hydride. The polymer was then purified by repeated precipitation from hot toluene into cold methanol and dried under vacuum. There was no change in peak shape or elution time by GPC compared to the precursor polymer. The phenanthrene content of hPS was calculated from UV−vis measurements using 9-hydroxymethylphenanthrene as a standard and was found to be 74 μmol/g.

Film Preparation. The block copolymer PS-*b(An)*-PBMA and hPS-*Phe* were each dissolved in toluene at 5 wt %. The two solutions were mixed to give solutions with $f_{phe} = w_{hPS}/(w_{hPS} + w_{PS-PBMA})$ of 0.05, 0.1, 0.2, 0.3, and 0.5, where w refers to the weights of each component. Since the densities of PS and PBMA are nearly identical (1.04 and 1.06 g/cm^3, respectively, at room temperature), f_{phe} is also approximately equal to the volume fraction of homopolymer in the blend. In addition, films with f_{phe} = 0 and 1.0 were prepared from the individual solutions. A first set of films was prepared by drying these mixtures in open air on quartz plates and then annealed at 140 °C for 4 h. The fluorescence of these films contains, in addition to the emission from the phenanthrene, an emission from the polymers themselves. To subtract the background emission from the signal, a second set of samples was prepared in a more controlled fashion. A gastight syringe was used to measure 50 μL of each solution and spread them onto quartz plates (2.5 cm × 2.5 cm × 0.1 cm). The solutions were then dried very slowly at room temperature in a closed box equipped with a small release hole in the presence of a reservoir of toluene in order to minimize the drying rate. After the films were dry (typically this took 48 h, but we removed the samples from the box only after a week), we annealed them at 90 °C for 2 h under vacuum. Fluorescence decay profiles of each film were measured. Then each film was annealed again for 4 h at 140 °C under vacuum.

Fluorescence Decay Measurements. Fluorescence decay profiles were measured by the single-photon-timing technique. The samples were excited at λ_{ex} = 300 nm, and phenanthrene fluorescence was detected at λ_{em} = 350 nm. A band-pass filter 350 ± 5 nm was used to eliminate all background from anthracene emission. The first set of samples was measured in a quartz tube where sample orientation was selected to obtain the maximum intensity. The second set of samples was measured in a goniometer sample holder. The films were positioned at 45 ± 1° from the excitation beam in such a way that the light reflected off the front surface of the film was directed away from the collection optics. Fluorescence was observed through the quartz substrate from the back of the film. The excitation and emission slits were fully opened for all the measurements, which lasted from 20 to 100 min, according to the concentrations of donor and acceptor in the films.

Energy Transfer Analysis. Direct nonradiative energy transfer (DET) takes place between a donor and an acceptor with a rate $w(r)$ that decreases with the sixth power of the distance r between the centers of the transition dipoles of the donor and the acceptor[17,19]

$$w(r) = \frac{3}{2}\frac{\kappa^2}{\tau_D}\frac{R_0^6}{r^6} \tag{1}$$

R_0 is the characteristic energy transfer distance (Förster radius), and τ_D is the unquenched lifetime of the donor. The term κ^2 is the orientation factor, which takes the value $^2/_3$ for rapidly reorienting dipoles and 0.47 for a random distribution of immobile donor and acceptor dipoles.[17b] For the phenanthrene and anthracene derivatives we examine here, R_0 = 2.3 nm.[29]

The quantum efficiencies of energy transfer, ϕ_{ET}, are defined by the expression

$$\phi_{ET} = 1 - \frac{\int_0^\infty I_D(t)\,dt}{\int_0^\infty I_D^0(t)\,dt} = 1 - \frac{F}{F^0} \tag{2}$$

where $I_D(t)$ refers to the normalized donor decay profile following a delta-pulse excitation for an experiment carried out in the presence of anthracene and $I_D^0(t)$ to the decay of a film containing only Phe. The time integral of $I_D(t)$ is equal to the fluorescence intensity F, and F^0 is the fluorescence intensity in the absence of acceptor. Measured decay profiles $I_{meas}(t)$ differ from $I_D(t)$ because of the instrument response function. This relationship is given in the following expression, where $Lamp(t')$ is the instrument response function.

$$I_{meas}(t) = I_0 \int I_D(t - t')\, Lamp(t')\, dt' \tag{3}$$

The mimic lamp profile, used for the convolution analysis,[30] was obtained by exciting a solution of *p*-terphenyl in aerated cyclohexane (lifetime: 0.96 ns). Individual $I_D(t)$ decays were fitted to a sum of up to three exponential terms, and then the integrals were calculated from the fitting parameters.

Results and Analysis

Morphology of PS-*b*-PBMA Block Copolymers and of Their Blends with hPS. The morphology of PS−PBMA block copolymers was first studied by Russell and co-workers,[31] using SAXS and dynamic rheological measurements. They reported that, depending on the molecular weight, these copolymers exhibit both an upper and a lower critical order transition. Recently, Schubert et al. described TEM and specular neutron reflectivity (SNR) experiments on symmetric PS−PBMA samples.[26] They found by TEM that a nondeuterated sample of M_w = 278 000 (f_{ps} = 0.5) cast from toluene solution and annealed at 150 °C exhibits a lamellar morphology. For this sample, they report a domain spacing of 60 nm and a PS block width of 33 nm. The deuterated sample (PSd-*b*-PBMA) of M_w = 248 000 (f_{ps} = 0.5) gave a comparable value of the period length (62 nm). From SNR experiments on the deuterated sample they obtained an interface thickness of approximately

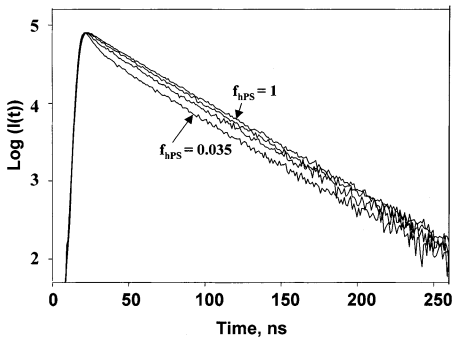

Figure 1. Experimental fluorescence decay curves for blends of PS-*b(An)*-PBMA (M_{PS} = 92 000, M_{PBMA} = 91 000) and phenanthrene-labeled PS homopolymer (M = 100 000) for f_{hPS} = 0.035, 0.08, 0.15, and 1.0. For comparison purposes, the decay curves were normalized at their maximum intensities. Films were excited at λ_{ex} = 300 nm, and the emission was detected at λ_{em} = 350 ± 5 nm.

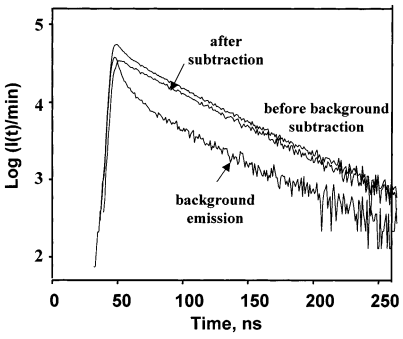

Figure 2. Absolute fluorescence decay curves, plotted logarithmically against time for films prepared from hPS-*Phe* (M = 100 000) and PS-*b(An)*-PBMA (M_{PS} = 92 000, M_{PBMA} = 91 000) at f_{hPS} = 0.035. The *y*-axis refers to the intensity counts divided by the measurement time. The top curve refers to the measured decay. The lower curve is the measured decay of an optically matched sample of pure PS-*b(An)*-PBMA, measured for an identical period of time. This curve represents background emission from the PS portion of the block copolymer. The middle curve is the corrected decay curve after subtraction of the background emission.

8.4 nm at 151 °C and 7.7 nm at 140 °C. More recently, Schubert[32] reported a period length of 41.4 nm and an interface thickness of 8.4 nm at 151 °C for a sample of M_w = 148 000 (f_{ps} = 0.5). We prepared our samples in a similar fashion and annealed them at 90 and 140 °C. Our copolymer has an intermediate molecular weight (M_w = 183 000). We anticipate a lamellar morphology for our samples, with a lamellar spacing close to 50 nm.

The interpretation of our fluorescence results depends on whether the addition of homopolymer alters the copolymer morphology. For hPS added to symmetric PS-*b*-PI block copolymer, Hashimoto and co-workers[8] found that the lamellar morphology persisted for blends containing up to 20% of hPS. When the hPS exceeded 35%, the morphology changed to hexagonally packed cylindrical microdomains. Winey et al. obtained similar results for the same system involving longer hPS chains.[9] Other researchers reported similar behavior for the PS−P2VP/hPS system.[15] We conclude that, for blends of hPS−Phe with PS-*b(An)*-PBMA containing up to 20 wt % homopolymer, the morphology will likely remain lamellar. Thus, we assume a lamellar morphology in our NSCF calculations.

Analysis of Fluorescence Decays. In Figure 1, we show phenanthrene fluorescence decay profiles for hPS-*Phe* in PS-*b(An)*-PBMA blends with f_{hPS} ranging from 0.035 to 0.15 and neat homopolymer (f_{hPS} = 1). The phenanthrene decay $I_D(t)$ in the pure hPS-*Phe* film fits well to an exponential function with τ_D = 43.69 ns. When mixed with PS-*b(An)*-PBMA, the $I_D(t)$ profile deviates from a single-exponential form. Since the Phe-labeled homopolymer exhibits a simple exponential decay, it is tempting to assign all deviation from an exponential form to energy transfer in the system. This turns out to be incorrect for reasons to be described in detail below. From this erroneous perspective, one would calculate DET efficiencies as high as 90% for samples containing only traces of hPS-*Phe*, suggesting preferential localization of the homopolymer in the block copolymer interface.

Polystyrene has a weak absorption at 300 nm and a weak fluorescence at 350 nm. In hPS−Phe, the high loading of Phe groups competes effectively with PS for the incident light, and its relatively intense fluorescence makes the emission from PS negligible. In mixtures with PS-*b(An)*-PBMA, background fluorescence from the PS in the block copolymer makes a significant contribution to the overall signal. For example, when a film of pure PS-*b(An)*-PBMA is excited at 300 nm and its emission monitored at 350 nm, we find a fast decay similar to that observed in samples containing low f_{hPS}. This signal must be subtracted as background. To proceed, we prepared optically flat polymer film samples of essentially identical thickness and mounted them on a goniometer in the sample chamber of the fluorescence decay apparatus. Decay profiles were measured both for donor + acceptor-containing films and for films for which only background fluorescence can be detected. The decay representing the background was measured with the pure An-labeled block copolymer (f_{hPS} = 0). The emission intensities were then normalized to the measurement time for the Phe-containing film. The normalized background decay was subtracted from the normalized sample measurements (Figure 2). We refer to the decay profiles with the background subtracted as "corrected" decays.

Once the background has been subtracted, the corrected decays can be fitted to a single-exponential function. The only indication of energy transfer is that the lifetimes calculated from the decay profiles are smaller than that obtained for the hPS−Phe sample itself (τ_D = 43.69 ns). In the hypothetical situation of a single separation distance r, the donor fluorescence intensity $I_D(t)$ would decrease exponentially with a rate $1/\tau = 1/\tau_D + w(r)$. We expect a distribution of donor−acceptor distances and nonexponential decays. When almost all the donors are far removed from acceptors, the deviation from exponential becomes too small to fit uniquely with a multiple parameter fit. The signature of this situation is a decay profile that can be fitted to a single exponential term with a lifetime marginally shorter than the unquenched lifetime. The quality of these fits to the corrected $I_D(t)$ profiles is illustrated by the random distribution of their residuals shown in Figure 3.

Simple exponential decays can be fitted with impressive precision. Each decay profile consists of 240 channels of data, with 10 000 counts in the maximum channel. Simulations in our group for nonexponential decays have shown that the area under a decay profile can be calculated with a precision better than 0.2%. Changes in lifetime of even 0.2 ns in 44 ns are reproducible and significant. In Figure 4, we show the

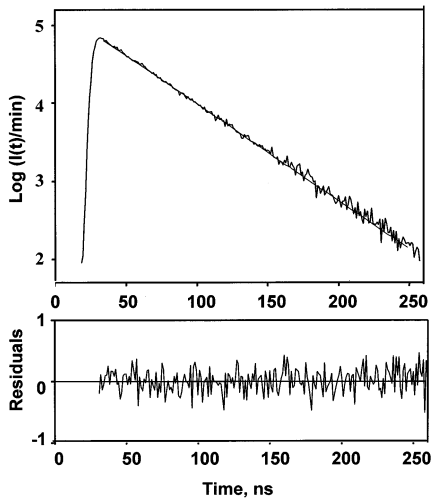

Figure 3. Corrected fluorescence decay curve for the blend with $f_{hPS} = 0.035$, fitted to a single-exponential profile. The weighted residuals for the fit are presented at the bottom of the figure.

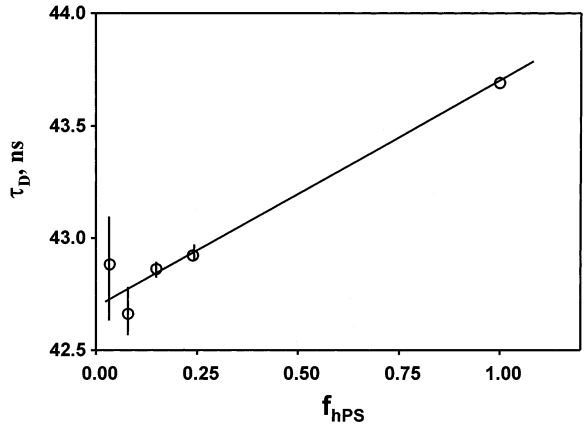

Figure 4. Lifetimes obtained by fitting the corrected fluorescence decays to a single-exponential model, plotted against f_{hPS}. The blends were cast from toluene as described in the text and annealed at 90 °C for 1 h.

variation of the phenanthrene lifetime plotted against f_{hPS}. The error bars represent one standard deviation and are calculated from a minimum of three measurements on individual samples. The larger error bars at low values of f_{hPS} arise as a consequence of subtracting the background signal from the measured decay. We find that the Phe lifetime increases with f_{hPS} from 42.6 ns for $f_{hPS} = 0.09$ to 42.9 ns for $f_{hPS} = 0.26$. We also note that these lifetimes are not much smaller than that of the pure hPS ($\tau_D = 43.69$ ns).

The preceding results indicate a very limited extent of energy transfer from Phe in hPS-*Phe* to the An in PS-*b(An)*-PBMA. In Figure 5 we show that for films annealed at 90 °C values of Φ_{ET} are on the order of 0.02. The characteristic DET distance R_0 for the Phe/An pair is approximately 2.3 nm. The probability of energy transfer becomes negligible as the donor−acceptor separation exceeds about $1.8R_0$. Assuming that Phe is a tracer for hPS-*Phe*, this implies that less than 2% of the hPS is located within 4 nm of the junctions of the block copolymer. These films were cast from a common good solvent for all of the components (toluene) and annealed at a temperature (90 °C) just below the glass transition of PS.

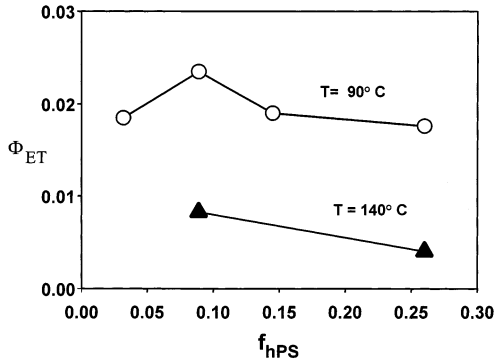

Figure 5. Values of the quantum efficiency of energy transfer Φ_{ET} calculated from corrected $I_D(t)$ profiles, plotted against f_{hPS} for blends cast from toluene solution and annealed for 1 h at 90 °C (open circles), and then at 140 °C (filled triangles).

The films were then annealed at 140 °C for 4 h (above the glass transition of PS) and rapidly cooled to room temperature. All of the corrected decays for these samples exhibit good fits to a single-exponential profile, with randomly distributed residuals. The lifetime of the pure hPS-*Phe* does not change upon annealing, but the lifetimes of the blends increase for all values of f_{hPS}: to 43.3 ns for $f_{hPS} = 0.09$ and to 43.5 ns for $f_{hPS} = 0.26$. The corresponding Φ_{ET} values decreased to less than 0.008 for $f_{hPS} = 0.09$ and to 0.004 for $f_{hPS} = 0.26$ (Figure 5). While the samples annealed at 90 °C may have been trapped in a metastable state, a more likely explanation is that a higher χ value at 140 °C led to further demixing of the homopolymer and block copolymer. After this second annealing, more than 99% of the hPS-*Phe* is located at least 4 nm from the interface.

As mentioned earlier, from SNR experiments the Stamm group found the PS−PBMA block copolymer to exhibit a broad segment distribution at the interface.[26,32] For the hypothetical situation where the distribution of the junctions is not altered by the presence of a small amount of homopolymer, approximately 5% of junctions will be located near the center of the PS phase. To obtain $\Phi_{ET} < 1\%$, essentially all of the hPS-*Phe* should be located between the PS domains of the block copolymer, i.e., in a dry-brush morphology.

We have mentioned that Shull and Winey[12] predicted a similar dry-brush structure for the PS−PI−hPS system for $N_{hPS} = 1.37N_{PS}$. The results of the systematic study of Vavasour and Whitmore[24] also imply that the homopolymer is excluded from the interface at high χ and large N_{hPS}.

Numerical Self-Consistent-Field Calculations. Numerical SCF calculations were carried out using the methodology described byVavasour and Whitmore.[24] For these calculations, we used the standard monomer definitions, which, for the almost perfectly compositionally symmetric copolymer in this paper, mean degrees of polymerization of 883 for the PS block and 640 for the PBMA block. For the hPS, which had a molecular weight of 100 000, this means $N_{hPS} = 960$.

Even recent and sophisticated block copolymer models tend to assume, for the sake of simplicity, that the statistical segment lengths of the two block copolymer components may be considered equal.[33,34] Almdal and co-workers[35] were the first to point out that the phase behavior of block copolymers could not be adequately understood without considering conformational asymmetry. Shortly afterward, Vavasour and Whitmore[36] introduced a conformational asymmetry parameter $\epsilon =$

$(\rho_{0B}b_B^2)/(\rho_{0A}b_A^2)$ for AB diblock copolymers, where ρ_{0P} (P = A or B) are the pure component densities and b_P are the Kuhn lengths for each block. They showed that, at the level of mean-field theory, the phase behavior depends on three quantities: χr_c, where r_c is an effective degree of polymerization, the relative volume fractions of each block, and the asymmetry parameter ϵ.

For an annealing temperature of 140 °C, we used values of ρ_{0PS} and ρ_{0PBMA} available from the papers by Quach and Simha[37] and Olabisi and Simha,[38] respectively. The Kuhn length of PS is well established: b_{PS} = 0.65 nm at 140 °C from Boothroyd and co-workers' small-angle neutron scattering (SANS) measurements on PS melts.[39] We employed this value both for hPS and the PS component of the block copolymer. For PBMA, we first attempted to "reproduce" the representative value 0.78 nm employed by the Stamm group[26a,c] for the segment length of PS-*b*-PBMA, on the assumption that geometric mean averaging would apply.[40] This gave b_{PBMA} = 0.94 nm and ϵ = 1.5, with PBMA having the longer effective step length (i.e., the statistical segment length if the PS and PBMA monomers were chosen to have the same volume.) In this first set of simulations, the χ parameter was taken to be 0.0098 (defined with reference to the monomer volume of polystyrene), as reported by Schubert and co-workers in 1998 for 140 °C.[26a]

With these input parameters, we first carried out calculations for the neat block copolymer. The results for the segment density distribution are shown in Figure 6a. In these calculations and for those described below, we employ a coordinate system in which the center of the PBMA microdomain defines the *xy* plane, and the interface lies parallel to this plane. The square data points are the result of the NSCF calculation, where the *x*-axis represents half a lamellar period broken up into 101 equidistant points. The solid line represents a hyperbolic tangent calculated with the Helfand−Tagami (HT) equation[40] as modified by Semenov[33] to allow for the effects of block connectivity and finite molecular weight. The HT and Semenov models are based on the assumption of strong segregation. There is little difference between the curves except at the extremes of the plot.

The NSCF calculations indicate that neither the center of the PS domain nor that of the PBMA domain is completely free of segments of the other polymer. In Figure 6b, we show the corresponding result for the junction distribution. There are two important features of this calculation. First, the junction distribution for the block copolymer is skewed from the symmetric as a consequence of the conformational asymmetry of the copolymer. Second, the junction distribution has a finite extension into the extremes of the PS and PBMA microdomains. This curve is noticeably different in shape than the hyperbolic secant form.[33,40]

To compare the interface width to that obtained in the experiments by the Stamm group, we need to define an interface thickness. If we take the reciprocal slope of the tangent to the curve at the inflection, we obtain a value of δ = 9.65 nm. This value is in reasonable agreement with the Stamm group's experimental results at 140 °C and the value of 9.2 nm at 151 °C reported more recently by Schubert [32] from specular neutron reflectivity experiments on a sample of M_w = 248 000. These experimental values have a certain ambiguity because of the need to correct for capillary waves or other sources of waviness at the interface. One of the unfortunate difficulties associated with interpreting neutron reflectivity data on polymer interfaces is that of trying to separate the contribution of the diffuse segment density profile at the interface from the contribution of low-amplitude sample undulations. Subtracting the effects of these undulations would reduce the effective width of the experimentally determined interface.

In Figure 7, we show the results of the computations for a mixture in which f_{hPS} = 0.02, employing χ = 0.0098 and b_{PBMA} = 0.94 nm as input parameters. We recall that the center of the PS microdomain defines the *xy* plane. We plot $\rho(z)$, representing the segment density of the PS homopolymer, and the junction distribution for the block copolymer in the direction normal to this plane. Here there are four important features of this calculation. (1) As in the case of the block copolymer itself, the junction distribution for the block copolymer is skewed from the symmetric. (2) The junction distribution extends into the extremes of the PS and PBMA microdomains. (3) The calculation shows that the PS homopolymer is preferentially localized at the center of the PS microdomain. (4) The distribution of the homopolymer segments overlaps appreciably with the block copolymer junctions. This simulation predicts the lamellar period to increase from 48.63 to 56.22 nm for f_{hps} ranging between 0.005 and 0.2.

At a later stage of our studies, we conducted some preliminary sensitivity analyses, employing a value of the χ parameter (0.0133 at 140 °C) proposed more recently by the Stamm group,[26c,d] along with a smaller Kuhn statistical segment length, 0.73 nm, for PBMA. (We calculated this value of b_{PBMA} using the approach described by Fredrickson and Helfand,[41] according to which, "in the spirit of a Flory−Huggins lattice theory", monomer number density is considered to be inversely proportional to the cube of the Kuhn length.) As a consequence of our choosing b_{PBMA} = 0.73 nm, the conformational asymmetry parameter decreased to ϵ = 0.9, so that PS had the larger effective step length. We found very little difference in the shapes of the curves for the segment density distributions, but with the smaller value of ϵ, the junction distributions tend to become more symmetric. The lamellar period for these parameters was somewhat smaller than for the first set, varying from 46.22 to 53.76 nm with f_{hPS}. This lower range occurred because of the smaller segment length for PBMA, which more than compensated for the larger χ.

We also examined the influence of the homopolymer on the width of the interface. When the interface thickness was taken as the reciprocal slope of the tangent to the inflection of the segment distribution profile, we found that δ decreased from 9.65 nm for the neat block copolymer to 9.59 nm with 2 vol % hPS present and to 9.39 nm with 20 vol % hPS. As an alternative estimate of the interface thickness, we examined the full width at half-height of the junction distribution. This value decreased from 11.34 nm with no hPS present to 11.31 and 11.16 nm respectively in the presence of 2% and 20% hPS.

Many authors who employed theoretical calculations to examine homopolymer−block copolymer blends invoked the narrow-interface approximation, neglecting any consequence of the homopolymer on the interface.

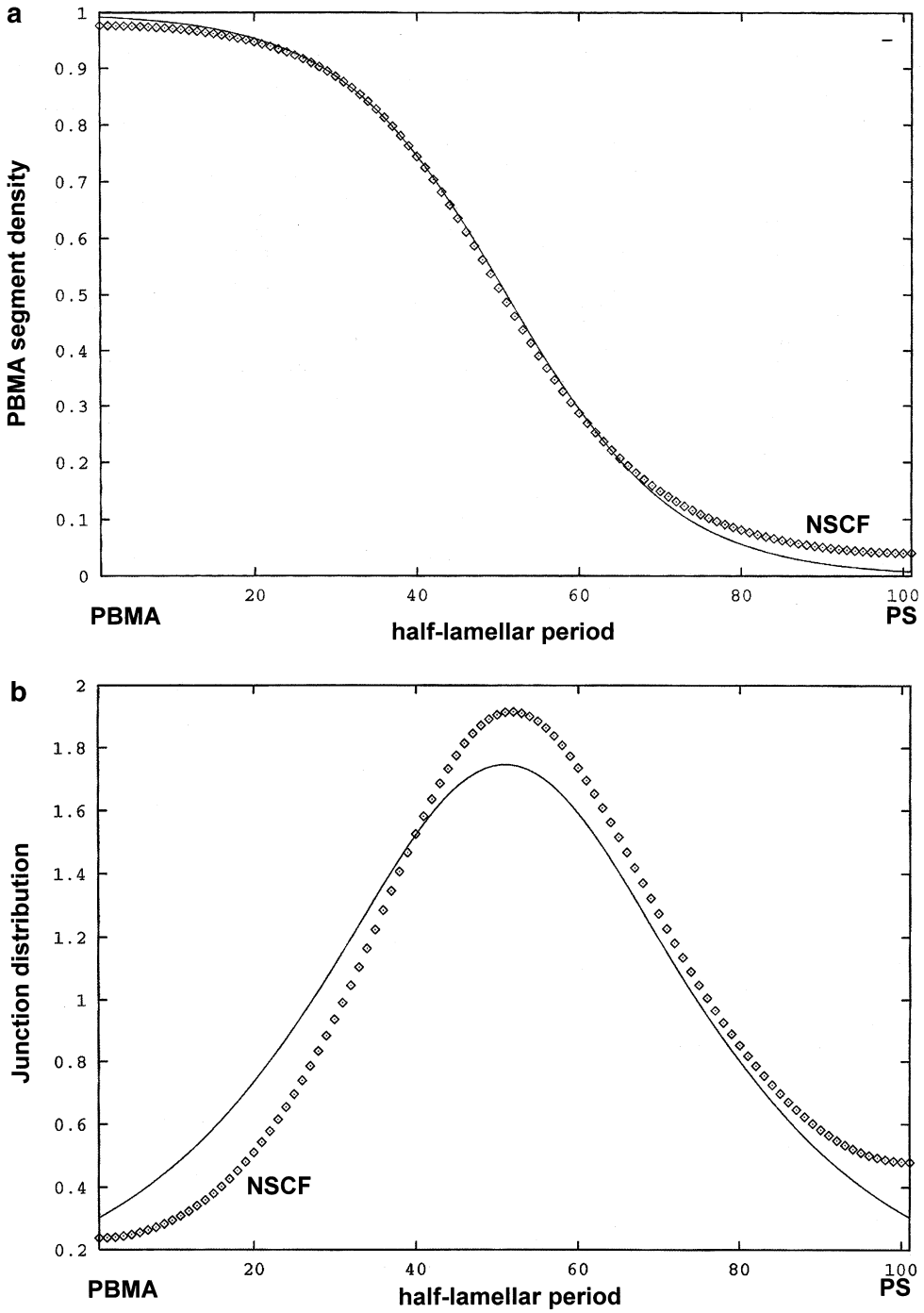

Figure 6. Result of self-consistent-field calculations on a dense melt corresponding to PS-*b*-PBMA (M_{PS} = 92 000, M_{PBMA} = 91 000) using parameters described in the text. In (a) we plot the calculated segment density profile of the PBMA block (□) and compare this result with a curve generated as a solution to the Helfand−Tagami−Semenov hyperbolic tangent expression with similar input parameters. In (b) we plot the distribution of copolymer junctions (□) and compare the result to a curve calculated with a hyperbolic secant junction distribution. In both plots, 2*L* is the lamellar spacing, and the *x*-axis scale is the distance from the center of the PBMA phase.

We know of only one experimental paper in which this matter was considered: an extensive study of the PS−PI + hPS system by the Hashimoto group,[8e] employing a combination of electron microscopy, SAXS, and SANS measurements. The latter experiments share with ours consideration of the case in which the molecular weight of the hPS was comparable to that of the PS block. These authors found that the thickness of the interface increased with the increase in the PS domain thickness, in the opposite direction to our NSCF results.

Comparison between the DET Experiments and the SCF Simulation. In this section we carry out a quantitative evaluation of the extent of energy transfer expected from a blend of hPS-*Phe* and PS-*b*(*An*)-PMMA satisfying the distributions predicted by the NSCF calculations as shown in Figure 7. We begin by estimating values of Φ_{ET} from the SCF profiles based upon a simple Perrin model of fluorescence quenching. We then evaluate Φ_{ET} from a more detailed analysis of the segment and junction distributions. These calculations

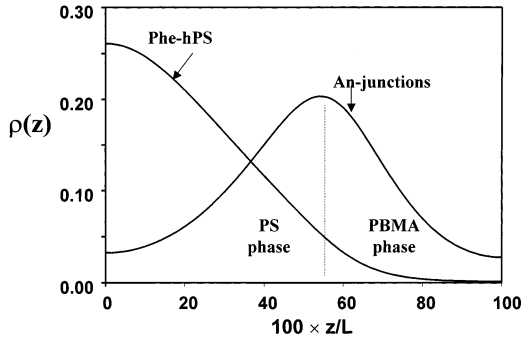

Figure 7. Results of self-consistent-field calculations of a blend consisting of hPS (M = 100 000) and PS-*b*-PBMA (M_{PS} = 92 000, M_{PBMA} = 91 000), with f_{hPS} = 0.02. The segment density profiles of the hPS (left) and the distribution of copolymer junctions (right) are plotted against the distance z from the center of the PS phase. $2L$ is the lamellar spacing.

assume that a small amount of homopolymer does not alter the lamellar structure of the blend. If swelling of the PS phase of the copolymer with hPS is isotropic, the lamellar period L will vary as $L_0(1 + f_{hPS})^{1/3}$. For f_{hPS} up to 0.2, the lamellar spacing will increase by less than 6%.

The Perrin Model of Fluorescence Quenching. The Perrin "active sphere" model[42] is an all-or-nothing static quenching model in which a quencher within the active quenching sphere (of radius R_p) quenches donor fluorescence, whereas a quencher outside this radius does not. In this model

$$\ln \frac{F^0}{F} = \frac{4\pi {R_p}^3}{3}[Q] \tag{4}$$

where [Q] is the molar concentration of quencher. For donors and acceptors in rigid media, fluorescence quenching can be fitted to the Perrin model, but it is described more correctly by the Förster model, which takes proper account of the distance dependence of $w(r)$ [$w(r) \sim (R_0/r)^6$]. The main difference between the exact form for DET and the Perrin model occurs in the vicinity of $r \approx R_0$, where the Perrin model overestimates $w(r)$ for $r \leq R_0$ and underestimates it for $r > R_0$. Values of R_p can be obtained from model experiments in which one examines polymer films containing low molecular weight dyes representative of the fluorophore and quencher of interest, and [Q] is the bulk quencher concentration in the film. These types of experiments show that the value obtained for R_p for a given pair of chromophores that undergo quenching by nonradiative energy transfer is very close in magnitude to, and slightly larger than, the value of R_0 obtained from the same experimental data by fitting the decays to the Förster model of DET for randomly distributed donors and acceptors in three dimensions.[43]

To compare experimental DET efficiencies with those predicted by the SCF calculations, we set $R_p = R_0 =$ 2.3 nm. The latter value is our current best estimate of the Förster radius for the phenanthrene−anthracene pair in our polymers.[29] We calculate values of Φ_{ET} from the expression

$$\phi_{ET} = \frac{\int C_D(z) \exp(-g(z))\, dz}{\int C_D(z)\, dz} \tag{5a}$$

$$g(z) = \pi N_A \int_{z-R_p}^{z+R_p} C_A(z')[{R_p}^2 - (z' - z)^2]\, dz' \tag{5b}$$

where N_A is Avogadro's number. The donor $C_D(z)$ and acceptor $C_A(z)$ concentration profiles are calculated from

$$C_D(z) = C_D^0 \rho_{hPS}(z)$$
$$C_A(z) = C_A^0 \rho_{junc}(z) \tag{6}$$

where C_D^0 and C_A^0 are the bulk-averaged number densities of phenanthrene and anthracene, respectively, in the homopolymer and copolymer. The terms $\rho_{hPS}(z)$ and $\rho_{junc}(z)$ represent the segment density profile of the homopolymer (hPS) and the distribution of the copolymer junctions (PS-*b*-PBMA) in the film, calculated from the SCF simulation.

In Figure 8 we plot values of Φ_{ET} calculated from the Perrin model using the SCF distribution profiles against f_{hPS} for the first set of parameters, χ = 0.0098. The Perrin−SCF calculation predicts a limiting value of Φ_{ET} = 0.15 for very small amounts of Phe-labeled PS homopolymer present in the film. Values of Φ_{ET} decrease from 0.15 to 0.09 for f_{hPS} ranging from 0.005 to 0.2. Using the second set of parameters with the larger χ, Φ_{ET} decreases from 0.10 to 0.056. In terms of this model less than 20% of the hPS is in the proximity of at least one junction. While the Perrin model gives a useful estimate of Φ_{ET}, it has several shortcomings. It does not take into consideration the exact form of the distance dependence of the rate of energy transfer, and it does not deal with the problems associated with the dipole−dipole orientation factor. A more realistic method of analysis requires the simulation of the fluorescence decays using the distribution profiles of the donors and acceptors.[30]

Energy Transfer from Simulated Fluorescence Decays. Klafter and Blumen[44] have described the general form for the donor fluorescence intensity $I_D(t)$ for situations where the donor and acceptor distribution profiles $C_D(z)$ and $C_A(z)$ are known.

$$I_D(t) = \exp(-t/\tau) \int C_D(r) \exp(-\varphi(r,t))\, dr \tag{7a}$$

$$\varphi(r,t) = \int C_A(r' - r)[1 - \exp(-w(r')t)]\, dr' \tag{7b}$$

The specific form for $I_D(t)$ for the situation where the chromophores are distributed along the normal to a planar surface was derived by Yekta et al.[45]

$$I_D(t) = \exp(-t/\tau_D) \int C_D(z) \exp[-g(z,t)]\, dz \tag{8a}$$

$$g(z,t) = 2\pi \int_0^\infty \langle C_A(r,z)\rangle [1 - \exp(-tw(r))] r\, dr \tag{8b}$$

$$\langle C_A(r,z)\rangle = N_A \int_{z-r}^{z+r} C_A(r')\, dr' \tag{8c}$$

$C_D(z)$ and $C_A(z)$ were calculated from eq 6 using the segment density profiles for hPS and the junction distribution profiles of PS-*b*-PBMA obtained from the SCF simulation. The integrals in eq 8c are evaluated analytically. The SCF calculation provides discretized profiles for $C_A(z)$, which we approximated as sums of shifted hyperbolic functions and quadratic polynomials:

$$C_A(i) \approx b_0 + b_1 \operatorname{sech}[b_2(i + b_3)] + b_4 i^2 + b_5 i \tag{9}$$

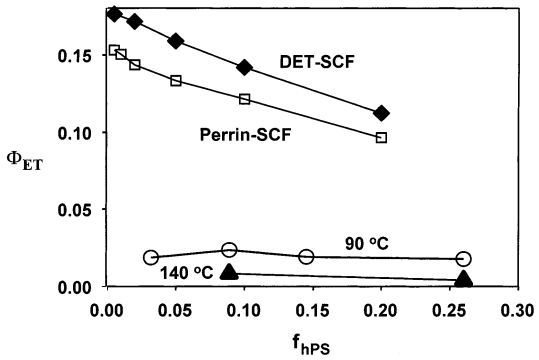

Figure 8. Quantum efficiency of energy transfer, Φ_{ET}, plotted against the volume fraction of Phe-labeled PS homopolymer in the film. Top-to-bottom. Decay simulation curve: values of Φ_{ET} calculated from the $I_D(t)$ decay curves simulated using eq 8 and the SCF predictions for the density distribution profile of hPS (MW = 100 000) and of the distribution of the PS-*b*-PBMA (MW_{PS} = 92 000, MW_{PBMA} = 91 000) junctions. Perrin−SCF simulation curve: values of Φ_{ET} calculated from the Perrin model, eq 4. DET results (open circles): experimental values for Φ_{ET} for blends annealed at 90 °C. DET results (filled triangles): experimental values for Φ_{ET} for blends annealed at 140 °C.

where $i = 1, 2, ..., 101$ represent 101 equidistant points across half of one lamellar period. Equation 9 gives a suitable approximation to the junction distribution, except in the center of the PBMA phase, where the homopolymer concentration is so low that the associated error in the calculated fluorescence intensity is negligible. We simulated the decays using $R_0 = 2.3$ nm and the lamellar spacings, polymer segment density profiles, and unction distributions from the SCF computations. These decays are noise-free profiles and do not take into account the instrument response time. To compare experiments and simulations, we convoluted $I_D(t)$ with an experimental lamp profile and added Poisson noise characteristic of the single-photon timing experiment.[30]

$$I_{sim}(t) = I_0 \int I_D(t - t')\, Lamp(t')\, dt' \qquad (10)$$

The $I_{sim}(t)$ profiles show two important characteristics: First, they decrease faster than the experimental decays $I_{meas}(t)$, for all values of f_{hPS}. Second, these decay profiles exhibit very poor fits to a single-exponential term. Both these results confirm that the SCF simulation predicts a much greater extent of energy transfer than that found by the DET experiments.

To calculate values of Φ_{ET}, $I_{sim}(t)$ were analyzed in the same manner as experimental decay profiles, using the mimic technique and trial functions for $I_D(t)$. The decays were fitted to a sum of two exponential terms and then integrated (cf. eq 2). The results are plotted as a function of f_{hPS} as the top curve in Figure 8. We see that Φ_{ET} decreases from 0.17 for $f_{hPS} = 0.005$ to 0.11 for $f_{hPS} = 0.2$. These values are slightly larger than those calculated from the Perrin model. We understand the difference between the two calculations from the choice of the quenching radius, where we arbitrarily assumed that $R_p = R_0$. Since the Perrin radius is slightly larger than the Förster radius, the use of 2.3 nm for both R_0 and R_p yields smaller values of Φ_{ET} for calculations based on the Perrin model.

The simulations predict the homopolymer to have limited miscibility within the interfacial region. The predicted decrease in Φ_{ET} with f_{hPS} implies that this miscibility also decreases with f_{hPS}; i.e., as more homopolymer is added, greater proportions segregate away from the interface.

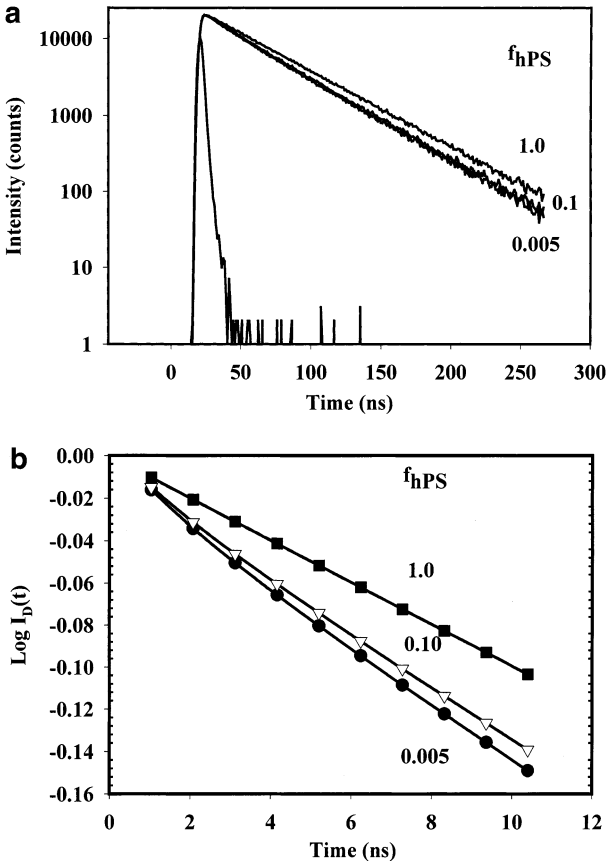

Figure 9. (a) Simulated single-photon counting decay curves for 0.5 wt % and 10.0 wt % hPS, with the exponential decay of pure hPS-*Phe* (τ_D = 43.69 ns) also shown, for comparison. (b) Noise-free delta-function excitation decays (first stage of the simulations) for each of the three curves of (a). For improved discrimination between the 0.5 and 10.0 wt % cases, simulated fluorescence intensities are shown for only the first 10 channels, i.e., up to t = 10.4 ns.

Figure 9 illustrates the simulated decays for two cases: 0.5 wt % hPS and 10.0 wt % hPS (the latter being a concentration similar to one of the experimental data points shown in Figure 8), with the exponential decay for τ_D = 43.69 ns shown for comparison. The 0.5 wt % hPS and 10.0 wt % hPS curves are similar to each other, with the small differences obscured by Poisson noise (Figure 9a). We see from the noise-free delta-function excitation curves (the first stage of each simulation[30]), shown for the first 10 channels, that there is more quenching at lower hPS content (Figure 9b).

While the SCF simulations predict Φ_{ET} values ranging from 10 to 17% at 140 °C, the DET experiments yield Φ_{ET} values that reach a maximum of 2% (Figure 8). Both results point to segregation of the homopolymer away from the interface of the PS−PBMA block copolymer, but the experiments indicate that the brush is much drier than predicted by these calculations. Since Φ_{ET} mirrors the distribution of homopolymer, this implies that the SCF calculations predict the solubility of hPS in the interface to be 5−6 times larger than that indicated by the experiments.

Discussion

Figure 3 illustrates that after correction for background emission the donor fluorescence decay curves for

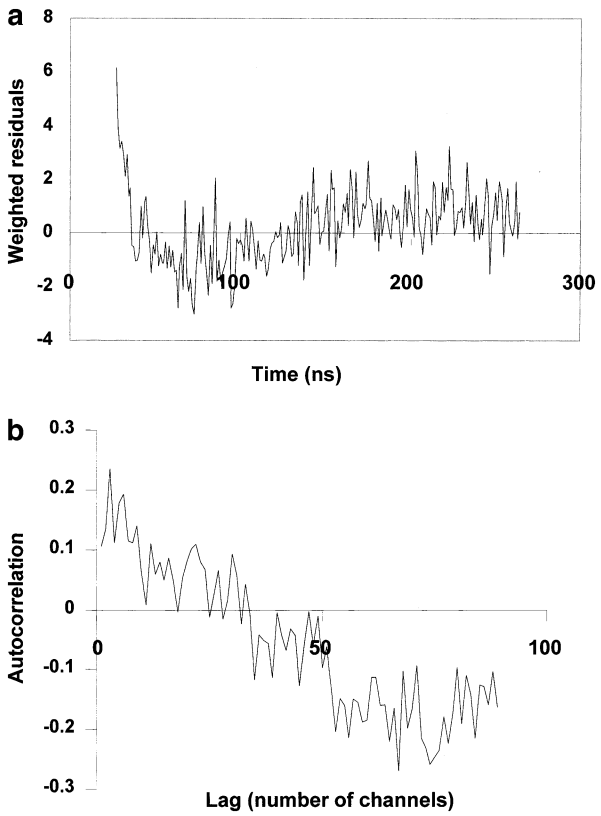

Figure 10. Weighted residual (a) and autocorrelation (b) plots resulting from force fitting a monoexponential decay model to a simulated SPC curve corresponding to the NSCF calculation with $\chi = 0.0098$ and $b_{PBMA} = 94.0$ nm for 10.0 wt % hPS blended into PS-*b*-PBMA.

blends of PS−PBMA + hPS show so little curvature that they give excellent fits to a single-exponential expression. The small values of the energy transfer efficiency calculated for this and other blends were obtained by comparing (eq 2) the fitted lifetimes for these blends to the unquenched lifetime of the pure hPS. To highlight the differences between the experimental results and the simulations, we show in Figure 10 that simulated fluorescence decay profiles cannot be fitted to a single-exponential form. We plot the weighted residuals and the autocorrelation of these residuals resulting from force fitting an exponential decay model to a simulated fluorescence decay curve corresponding to the NSCF calculation with $\chi = 0.0098$ and $b_{PBMA} = 0.94$ nm for 10.0 wt % hPS blended into PS-*b*-PBMA. The fit is poor and helps to emphasize our conclusion that the NSCF simulations, with our input parameters, predict a larger extent of energy transfer, associated with deeper penetration of the hPS into the PS brush of the block copolymer, than found in the experiments.

There are three possible origins of the difference between simulation and experiment. The first is the choice of spectroscopic parameters like R_0 used to compare the results of the NSCF calculations to experiments. The second is the choice of parameters used in the NSCF calculations, particularly χ and the statistical segment lengths. The third involves assumptions like incompressibility that are built into the NSCF calculation.

In calculating the energy transfer efficiency from the NSCF results, we used $R_0 = 2.3$ nm, which is the best estimate currently available for the phenanthrene−anthracene pair[29] in a polymer matrix. It is nevertheless clear that if R_0 were significantly smaller, the calculated efficiency of energy transfer would drop. Values of R_0 are determined from model compounds, which are intended to mimic the behavior of the chromophores attached to the polymer. Roller[46] in our group has been determining R_0 (and R_p) values for a series of phenanthrene and anthracene derivatives in polymer matrices. For simple nonpolar dyes like Phe and An, the overlap integral tends to depend more on the substituents on the dye than on spectral shifts associated with the medium. These experiments are in progress and will be described with other outstanding issues in a future publication. In the meantime, $R_0 = 2.3$ nm is the best estimate of R_0 for the experiments reported here.

There are a number of related, subtle features associated with these experiments. For example, if one uses spectroscopic methods to evaluate the overlap integral of the donor emission and acceptor absorption to calculate R_0, the choice of the proper orientation factor becomes an issue in calculating the magnitude of R_0. On the other hand, one can evaluate an effective R_0 directly from fluorescence decay measurements on model compounds dissolved in polymer matrices. Here one does not have to make assumptions about the orientation factor operating in those experiments. This effective R_0 value can be carried forward into the analysis of data for block copolymer−homopolymer blends. Orientation effects are unlikely to be a problem in the experiments reported here, since there is no reason to expect a preferred orientation for the Phe groups attached to the hPS homopolymer in the blend.

The choice of system parameters used in the NSCF calculations raises a number of interesting questions, which are usefully discussed in the context of the NSCF results of Vavasour and Whitmore.[24] They explored the behavior of the blends from weak through to strong segregation regimes. In their comparisons with experiments on PS−PI, when they used the literature values of χ, the NSCF calculations predicted layer thicknesses for the neat copolymer that were less than observed, and the predicted effects of added homopolymer were in qualitative agreement with experiment, but characteristic of weakly segregated systems. However, when they used larger values of χ, the NSCF calculations produced a consistent picture of both the neat copolymer and the effects of added homopolymer, all in good agreement with experiment. It also turned out that the appropriate value of χ depended sensitively on the values of the statistical segment lengths, i.e., the conformational asymmetry parameter. The effects can be large. Literature values of χ for that system (PS−PI) range from 0.035 to 0.086. They found that they should use $\chi = 0.100$ for $\epsilon = 1$; for modest conformational asymmetry of $\epsilon = 1.3$, they found that χ should be increased by 40% to 0.142. Either of these choices produces a qualitative change in behavior, more characteristic of intermediate or strong segregation. Vavasour and Whitmore[24] postulated that the values of χ in the literature are small because they were extracted from experiments in which fluctuations may be important but that are not fully included in the theories used to interpret the measurements. In principle, a more reliable way to determine χ would be through measurements on systems in which fluctuations are not important.

The parameters used in the NSCF calculations include statistical segment lengths for the PS and PBMA

copolymer blocks and the hPS. Of these, the value of b_{PBMA} is problematic. The value of 0.94 nm that we employed in our initial calculations is probably a reasonable *upper bound*,[47] but the correct value may well be as low as 0.61 nm.[47,48] This wide range, $b_{PBMA} = 0.61-0.94$ nm, corresponds to very different conformational asymmetries, ranging from $\epsilon = 0.6$ to 1.5.

Turning to considerations of χ, we initially used the value of 0.0098 at 140 °C, reported by Schubert and coworkers in 1998.[26a] Later, the Stamm group obtained the formula $[\chi = (0.0243 \pm 0.0004) - (4.56 \pm 0.169)/T\,(K)]$[26c] for the temperature-dependent χ parameter, more consistent with the lower critical ordering temperature (LCOT) behavior of PS-*b*-PBMA. This expression gives $\chi = 0.0133$ at 140 °C, the other value we used. A recent evaluation[32,34] of specular neutron reflection (SNR) data on symmetric diblock copolymers of (deuterated) PS and PBMA suggests that this is a suitable range of χ values to consider.

There is evidence, however, that casts doubt on these values. Other experiments, employing an array of techniques, claim a strong dependence of $\chi_{PS-PBMA}$ on molecular weight.[49] We also note a 1996 review[50] of polymer blend thermodynamics, which gives $\chi_{PS-PBMA}$ as a function of temperature over the range 20−130 °C, based on SANS measurements by Hammouda and coworkers.[51] Extrapolation to our conditions (140 °C) would yield $\chi_{PS-PBMA} = 0.0183$, which is nearly 50% or 100% larger than the two values we used. From a theoretical perspective, Vavasour and Whitmore's results[24] suggest that the appropriate value of χ could be even larger, and furthermore, it might be very sensitive to the high uncertainty in b_{PBMA}.

Incidentally, the apparent conflict between Hammouda and co-workers' χ parameters[51] and the Stamm group results[26] may be a manifestation of a difficulty pointed out by Maurer and co-workers,[52] namely, that block copolymer theories do not account for chain stretching properly. This may have compromised the $\chi_{PS-PBMA}$ values reported by the Stamm group.

The assumption of incompressibility, built into the NSCF methods[24] we have employed, may not be realistic. Yeung et al.[53] suggested that, as in homopolymer blends, (micro)phase separation with increasing temperature is a consequence of a finite compressibility effect. In a similar vein, Russell and associates expressed doubt in a 1995 paper[54] that "assuming an incompressible system characterized by a positive segmental interaction parameter" would be proper for PS-*b*-PBMA.

The Stamm group[25b] carried out dynamic mechanical measurements on a series of PS−PBMA block copolymers with different block ratios. For each composition, they found two glass transitions. The higher T_g (100 °C) was independent of block copolymer composition and led them to infer that the PS domain consisted of essentially pure polystyrene. In contrast, the lower T_g increased from its value of 31 °C in pure PBMA to ca. 40 °C in the block copolymer sample with 40 vol % PS. From these results, the authors concluded that the other domain, away from the interface, was a PBMA-rich domain and not a pure PBMA domain. To the extent that this conclusion is correct, it suggests that future experiments examining energy transfer from donor-labeled PBMA homopolymer to acceptors at the junction of PS−PBMA would be interesting. Here one might find deeper penetration of the PBMA into the block copolymer brush. We will examine this situation in more detail in a forthcoming paper on PS−PBMA block copolymers.[55]

The most reasonable conclusion from the discussion presented above is that, with the parameters used in the NSCF simulations, they predict much "wetter" brushes in PS-*b*-PBMA/hPS blends than observed. One possible explanation is the values of the χ parameter and b_{PBMA}; in particular, larger values of χ would predict drier brushes, and such larger values would be consistent with earlier findings. They would also result in narrow interfaces. Such narrow interfaces would also need to be compared with experiment, a comparison that will need to consider the contributions of undulations of the interfaces in the experiments.

Acknowledgment. The authors thank NSERC Canada for their support of this research. R. Jérôme is grateful to the "Services Fédéraux des Affaires Scientifiques, Techniques et Culturelles" for financial support in the frame of the "Pôles d'attraction Interuniversitaires: 4-11: Chimie Supramoléculaire et Catalyse Supramoléculaire". The authors also acknowledge numerous stimulating discussions with R. Roller and J. Yang of the Chemistry Department, University of Toronto.

References and Notes

(1) Hamley, I. W. *The Physics of Block Copolymers*; Oxford University Press: New York, 1998.
(2) Bates, F. S.; Fredrickson, G. H. *Annu. Rev. Phys. Chem.* **1990**, *41*, 525.
(3) Stamm, M.; Schubert, D. W. *Annu. Rev. Mater. Sci.* **1995**, *25*, 325.
(4) (a) Likhtmann, A. E.; Semenov, A. N. *Macromolecules* **1997**, *30*, 7273. (b) Xi, H.; Milner, S. T. *Macromolecules* **1996**, *29*, 2404. (c) Matsen, M. W. *Macromolecules* **1995**, *28*, 5765. (d) Matsen, M. W. *Phys. Rev. Lett.* **1995**, *74*, 4225. (e) Semenov, A. N. *Macromolecules* **1993**, *26*, 2273. (f)Whitmore, M. D.; Smith, T. W. *Macromolecules* **1994**, *27*, 4673. (g) Whitmore, M. D.; Noolandi, J. *Macromolecules* **1985**, *18*, 657.
(5) Ferreira, P. G.; Ajdari, A.; Leibler, L. *Macromolecules* **1998**, *31*, 3994.
(6) Floudas, G.; Hadjichristidis, N.; Stamm, M.; Likhtmann, A. E.; Semenov, A. N. *J. Chem. Phys.* **1997**, *106*, 3318.
(7) Ptaszynski, B.; Terrisse, J.; Skoulios, A. *Makromol Chem.* **1975**, *176*, 3483.
(8) (a) Hashimoto, T.; Tanaka, H.; Hasegawa, H. *Macromolecules* **1990**, *23*, 4378. (b) Tanaka, H.; Hasegawa, H.; Hashimoto, T. *Macromolecules* **1991**, *24*, 240. (c) Tanaka, H.; Hashimoto, T. *Macromolecules* **1991**, *24*, 5713. (d) Koizumi, S.; Hasegawa, H.; Hashimoto, T. *Macromolecules* **1994**, *27*, 6532. (e) Koizumi, S.; Hasegawa, H.; Hashimoto, T. *Macromolecules* **1994**, *27*, 7893.
(9) (a) Winey, K. I.; Thomas, E. L.; Fetters, L. J. *Macromolecules* **1991**, *24*, 6182. (b) Winey, K. I.; Thomas, E. L.; Fetters, L. J. *Macromolecules* **1992**, *25*, 2645.
(10) Jeon, K.-Y.; Roe, R. J. *Macromolecules* **1994**, *27*, 2439.
(11) Leibler, L. *Makromol. Chem. Macromol. Symp.* **1988**, *16*, 1.
(12) Shull, K. R.; Winey, K. I. *Macromolecules* **1992**, *25*, 2637.
(13) (a) Mayes, A. M.; Russell, T. P.; Satija, S. K.; Majkrzak, C. F. *Macromolecules* **1992**, *25*, 6523. (b) Mayes, A. M.; Johnson, R. D.; Russell, T. P.; Smith, S. D.; Satija, S. K.; Majkrzak, C. F. *Macromolecules* **1993**, *26*, 1047. (c) Shull, K. R.; Mayes, A. M.; Russell, T. P. *Macromolecules* **1993**, *26*, 3929.
(14) Orso, K. A.; Green, P. F. *Macromolecules* **1999**, *32*, 1087.
(15) (a) Matsushita, Y.; Torikai, N.; Mogi, Y.; Noda, I.; Han, C. C. *Macromolecules* **1993**, *26*, 6346. (b) Matsushita, Y.; Torikai, N.; Mogi, Y.; Noda, I.; Han, C. C. *Macromolecules* **1994**, *27*, 4566. (c) Torikai, N.; Takabayashi, N.; Noda, I.; Koizumi, S.; Morii, Y.; Matsushita, Y. *Macromolecules* **1997**, *30*, 5698.
(16) Auroy, P.; Mir, Y.; Auvray, L. *Phys. Rev. Lett.* **1992**, *69*, 93.
(17) (a) Förster, T. *Discuss. Faraday Soc.* **1959**, *27*, 7. (b) Baumann, J.; Fayer, M. D. *J. Chem. Phys.* **1986**, *85*, 4087.
(18) Birks, J. B. *Photophysics of Aromatic Molecules*; Wiley-Interscience: New York, 1970.

(19) For reviews of the use of energy transfer to study polymers, see: Morawetz, H. *Science* **1988**, *240*, 172.
(20) (a) Rharbi, Y.; Winnik, M. A. *Macromolecules* **2001**, *34*, 5238. (b) Tcherkasskaya, O.; Ni, S. R.; Winnik, M. A. *Macromolecules* **1996**, *29*, 4241. (c) Tcherkasskaya, O.; Spiro, J. G.; Ni, S.; Winnik, M. A. *J. Phys. Chem.* **1996**, *100*, 7114.
(21) (a) Feng, J.; Winnik, M. A. *Macromolecules* **1997**, *30*, 4324. (b) Farinha, J. P. S.; Vorobyova, O.; Winnik, M. A. *Macromolecules* **2000**, *33*, 5863.
(22) Matsen, M. W. *Macromolecules* **1995**, *28*, 5765.
(23) Banaszak, M.; Whitmore, M. D. *Macromolecules* **1992**, *25*, 2757.
(24) Vavasour, J. D.; Whitmore, M. D. *Macromolecules* **2001**, *34*, 3471.
(25) (a) Weidisch, R.; Michler, G. H.; Arnold, M.; Hofmann, S.; Stamm, M.; Jerôme, R. *Macromolecules* **1997**, *30*, 8078. (b) Weidisch, R.; Michler, G. H.; Fischer, H.; Arnold, M.; Hofmann, S.; Stamm, M. *Polymer* **1999**, *40*, 1191.
(26) (a) Schubert, D. W.; Weidisch, R.; Stamm, M.; Michler, G. H. *Macromolecules* **1998**, *31*, 3743. (b) Schubert, D. W.; Abetz, V.; Stamm, M.; Hack, T.; Siol, W. *Macromolecules* **1995**, *28*, 2519. (c) Weidisch, R.; Stamm, M.; Schubert, D. W.; Arnold, M.; Budde, H.; Höring, S. *Macromolecules* **1999**, *32*, 3405. (d) Schubert, D. W.; Stamm, M.; Müller, A. H. E. *Polym. Eng. Sci.* **1999**, *39*, 1501.
(27) (a) Hruska, Z.; Vuillemin, B.; Riess, G.; Katz, A.; Winnik, M. A. *Makromol. Chem.* **1992**, *193*, 1987. (b) Ni, S.; Zhang, P.; Wang, Y.; Winnik, M. A. *Macromolecules* **1994**, *27*, 5742.
(28) Camps, M.; Chatzopoulos, M.; Camps, J.-M.; Montheard, J.-P. *J. Macromol. Sci., Rev. Macromol. Chem. Phys.* **1987−88**, *C27* (3&4), 505.
(29) (a) Wang, Y.; Zhao, C.-L.; Winnik, M. A. *J. Chem. Phys.* **1991**, *95*, 2143. (b) Duhamel, J.; Yekta, A.; Ni, S.; Khaykin, Y.; Winnik, M. A. *Macromolecules* **1993**, *26*, 6255.
(30) Yekta, A.; Spiro, J. G.; Winnik, M. A. *J. Phys. Chem. B* **1998**, *102*, 7960.
(31) (a) Russell, T. P.; Karis, T. E.; Gallot, Y.; Mayes, A. M. *Nature (London)* **1994**, *368*, 729. (b) Karis, T. E.; Russell, T. P.; Gallot, Y.; Mayes, A. M. *Macromolecules*, **1995**, *28*, 1129.
(32) Schubert, D. W. *Macromol. Symp.* **2000**, *149*, 257.
(33) Semenov, A. N. *Macromolecules* **1993**, *26*, 6617.
(34) Matsen, M. W.; Bates, F. S. *Macromolecules* **1996**, *29*, 1091.
(35) Almdal, K.; Koppi, K. A.; Bates, F. S. *Macromolecules* **1992**, *25*, 1743.
(36) Vavasour, J. D.; Whitmore, M. D. *Macromolecules* **1992**, *25*, 5477.
(37) Quach, A.; Simha, R. *J. Appl. Phys.* **1971**, *42*, 4592.
(38) Olabisi, O.; Simha, R. *Macromolecules* **1975**, *8*, 206.
(39) Boothroyd, A. T.; Rennie, A. R.; Wignall, G. D. *J. Chem. Phys.* **1993**, *99*, 9135.
(40) Helfand, E.; Tagami, Y. *J. Polym. Sci., Part B: Polym. Lett.* **1971**, *9*, 741.
(41) Fredrickson, G. H.; Helfand, E. *J. Chem. Phys.* **1987**, *87*, 697.
(42) Lakowicz, J. R. *Principles of Fluorescence Spectroscopy*; Plenum: New York, 1983; pp 271−276.
(43) Yang, J.; Winnik, M. A. *Can. J. Chem.* **1995**, *73*, 1823.
(44) Klafter, J. M.; Blumen, A. *J. Chem. Phys.* **1984**, *80*, 875. (b) Blumen, A.; Klafter, J.; Zumofen, G. *J. Chem. Phys.* **1986**, *84*, 1397.
(45) Yekta, A.; Duhamel, J.; Winnik, M. A. *Chem. Phys. Lett.* **1995**, *235*, 119.
(46) Roller, R.; Winnik, M. A., to be submitted.
(47) *Polymer Handbook*, 4th ed.; Brandrup, J., Immergut, E. H., Grulke, E. A., Eds.; John Wiley & Sons: New York, 1999; p VII−50.
(48) Helfand, E.; Sapse, A. M. *J. Chem. Phys.* **1975**, *62*, 1327.
(49) Fischer, H.; Weidisch, R.; Stamm, M.; Budde, H.; Höring, S. *Colloid Polym. Sci.* **2000**, *278*, 1019.
(50) Balsara, N. P. In *Physical Properties of Polymers Handbook*; Mark, J. E., Ed.; American Institute of Physics: New York, 1996; pp 257−268.
(51) Hammouda, B.; Bauer, B. J.; Russell, T. P. *Macromolecules* **1994**, *27*, 2357.
(52) Maurer, W. W.; Bates, F. S.; Lodge, T. P.; Almdal, K.; Mortensen, K.; Fredrickson, G. H. *J. Chem. Phys.* **1998**, *108*, 2989.
(53) Yeung, C.; Desai, R. C.; Shi, A.-C.; Noolandi, J. *Phys. Rev. Lett.* **1994**, *72*, 1834.
(54) Karis, T. E.; Russell, T. P.; Gallot, Y.; Mayes, A. M. *Macromolecules* **1995**, *28*, 1129.
(55) Rharbi, Y.; Spiro, J. G.; Yang, J.; Winnik, M. A.; Vavasour, J. D.; Whitmore, M. D.; Jérôme, R., to be submitted.

MA020962L